International Journal on Recent and Innovation Trends in Computing and Communication
ISSN: 2321-8169 Volume: 10 Issue: 10
DOI: https://doi.org/10.17762/ijritcc.v10i10.5732
***Article Received**: 28 July 2022 **Revised**: 05 September 2022 **Accepted**: 12 September 2022*

Prediction of Cardiovascular Diseases by Integrating Electrocardiogram (ECG) and Phonocardiogram (PCG) Multi-Modal Features using Hidden Semi Morkov Model

Prasadgouda B Patil[1, *], Dr.Vijay Bhaskar Reddy[2] and Dr.Ashokumar P S[3]
[1]Research Scholor, Department of Computer CSE, Reva University, Bengaluru, India.
[2]Professor, School of Computer Science and Engineering, REVA University, Bengaluru, India, E-mail: bhaskarreddy.pv@reva.edu.in
[3]Professor and Head Department of Computer CSE, HKBK College of Engineering, Bangalore, India, E-mail: ashokydit@gmail.com
*Corresponding Author Email: prasad7515@gmail.com

Abstract

Because the health care field generates a large amount of data, we must employ modern ways to handle this data in order to give effective outcomes and make successful decisions based on data. Heart diseases are the major cause of mortality worldwide, accounting for 1/3th of all fatalities. Cardiovascular disease detection can be accomplished by the detection of disturbance in cardiac signals, one of which is known as phonocardiography. The aim of this project is for using machine learning to categorize cardiac illness based on electrocardiogram (ECG) and phonocardiogram (PCG) readings. The investigation began with signal preprocessing, which included cutting and normalizing the signal, and was accompanied by a continuous wavelet transformation utilizing a mother wavelet analytic morlet. The results of the decomposition are shown using a scalogram, and the outcomes are predicted using the Hidden semi morkov model (HSMM). In the first phase, we submit the dataset file and choose an algorithm to run on the chosen dataset. The accuracy of each selected method is then predicted, along with a graph, and a modal is built for the one with the max frequency by training the dataset to it. In the following step, input for each cardiac parameter is provided, and the sick stage of the heart is predicted based on the modal created. We then take measures based on the patient's condition. When compared to current approaches, the suggested HSMM has 0.952 sensitivity, 0.92 specificity, 0.94 F-score, 0.91 ACC, and 0.96 AUC.

Keywords- cardiovascular diseases, machine learning, prediction, feature extraction, wavelet transform, kalman filter

Introduction

Cardiovascular diseases (CVDs) represent the most prevalent chronic illnesses worldwide, accounting for the leading cause of morbidity and mortality during the previous 10 years [1]. Based on WHO, almost 18 M patients die from CVDs every year, which accounts for 32percent of total of deaths globally. As a result, CVD cases are increasing at an alarming rate, and by 2k30, annual mortality rate will have risen to 22.2 million individuals [2]. Centers for Disease Control and Prevention analysis shows that the death rate will rise. It was stated that one person died every forty seconds as a result of CVDs. [3]. CVDs have also been identified as primary reason of death in Egypt during past thirty yrs., accounting for 46.2percent of all mortality cases as of 2k17 [4]. CVDs cover a variety of heart and blood vessel problems [5]. 4 of 5 CVD deaths were caused by strokes or heart attacks. As a result, heart disease is the most lethal chronic disease, and its danger stems from the disease's invisibility. It is not identified until signs of heart problems (or an attack) are observed [6]. Heart disease occurs when the heart fails to perform its regular role of giving blood towards other body parts due to a blockage of the coronary arteries, which are responsible for sending blood to the heart [7]. Regular heart disease signs are (1) shortness of breath, (2) weakness of the body, (3) disorientation, and (4) fainting. This illness risk is enhanced in those who have risk factors such as (1) an unhealthy lifestyle, (2) tobacco, (3) unfitness, (4) elevated BP, (5) a lack of exercises, and (6) an excessive bad cholesterols [8]. Early and precise prognosis of cardiac disease is critical for increasing survival and decreasing death. This will assist healthcare providers in making decisions by offering patients with a precise and effective diagnosis and treatment in order to save their lives. Machine intelligence is one strategy for early and reliable prediction of heart disease. This may be accomplished through the use of machine learning (ML) techniques and deep learning (DL) techniques [9].

International Journal on Recent and Innovation Trends in Computing and Communication
ISSN: 2321-8169 Volume: 10 Issue: 10
DOI: https://doi.org/10.17762/ijritcc.v10i10.5732
***Article Received**: 28 July 2022 **Revised**: 05 September 2022 **Accepted**: 12 September 2022*

The 2 most popular and successful methods in the first diagnosis of heart disorders are heart sound auscultation as well as electrocardiogram (ECG). The mechanical and electrical activity of the heart can be reflected by their signal waveforms, phonocardiogram (PCG) and ECG. PCG signals shows physiological/pathological states of cardiac vessels, allowing structural heart disease (SHD) is to be diagnosed. The ECG can aid in the detection of disorders related to impulse conduction, like arrhythmias, coronary heart disease, heart attacks, and so on [10The regular cardiac cycle is reliant on the interaction of nerve currents with electromechanical contraction of the atria and ventricles of the heart. A random nerve impulse in the sinoatrial (SA) node (shown as a P wave on an ECG) initiates the process, that subsequently propagates towards the atrioventricular (AV) nodes, allowing cardiac atria to relax enabling plasma to be transported through into blood vessels, and ventricular depolarization (represented as a QRS complex on an ECG) to begin [11]. When the ventricular pressure exceeds the atrial pressures, the atrioventricular valves collapse. The heart valves are repolarized (shown as a T wave on a PCG) and relaxed when the blood is pumped out. S2 on PCG is caused by the closing of semilunar valves. As a result, the PCG and ECG are tightly connected in time. It is critical to separate S1 from S2 in order to properly utilize the PCG's diagnostic power. All of the proposed segmentation techniques may be broadly classified as follows: 1) ECG reference techniques rely on the R-peak with T wave to pinpoint the location [12]. It necessitates simultaneously monitoring of both ECG as well as PCG, yet its performance is robust and computationally efficient. 2) Envelope-based approaches are more widely utilized in non-ECG-based segmentation. They utilize signal energy to conduct morphological transformations, However, with in existence of noisy environment and whispers, their performance diminishes. 3) Space - time predictor variables methods use time and frequency domains features of heartbeat sounds, whispers, and noise to divide heart rhythm; 4) Adaptive filtering Classification methods based are also an evolution of space - time parameter settings methodologies. They will dissect the signals such that cardiac sounds are highlighted while disturbances and noises are suppressed[13]. The fundamental problem of curve let segmentation is determining the best filtration, breakdown level, and sub-bands to recognize recordings and disturbances. 5) In recent times, Hidden Markov algorithms were also employed for segmentation, yielding outstanding results with low signal-to-noise ratios. There is currently no commonly accepted optimum PCG segmentation method, although with continuous ECG recordings, because of resilience. References show that multi-modal characteristics are useful in predicting CVDs. While facing high features in a multi-modal situation, however, feature selection stages are unavoidable. As a result, we require an efficient solution to tackle the dimension reduction problem. The aim of this research is to create a novel model that can reliably predict CVDs by integrating ECG and PCG. It is extremely useful for diagnosis and management of CVDs. The following are the primary contributions of this paper:

- To predict CVDs, a new model depending both on ECG and PCG data is developed.
- We generate 2 systems to encode ECG as well as PCG signals. Deep-coding characteristics of ECG and PCG are then computed and shown using boxplots and correlations.
- To acquire a greater representation of data, multi-modal feature extraction using matching is used throughout the feature dimension reduction procedure.
- Reporting cutting-edge performance indicators in comparison to other relevant research and methodologies.

The remaining study is organized as follows: Segment 2 addresses various current research investigations, Section 3 offers technique and techniques, Segment 4 displays the experiment results and discussion, Segment 5 concludes with the conclusions including prospective studies.

Related works

The upcoming section provides an overview of existing research and study papers on cardiovascular disease detection as well as forecasting approaches based on various types of medical data. The relevant research are divided into two categories: multimodal feature extraction studies and machine learning-based prediction studies.

Survey on multimodal feature extraction

[14] created the Synchronized ECG and PCG Database for People with Left Ventricular Dysfunction (SEP-LVDb), that includes 1046 synchronized ECG or PCG records involving patients who had low (n = 107) and healthy (n = 699) LVEF. There have been 173 and 873 records from the decreased and typical LVEF groups, correspondingly. Then, by combining PCG with ECG information, we created a concurrent multifunctional strategy for LVD assessment.

[15] describe a non-invasive approach for monitoring FHR which uses electro-cardio graphic (ECG) as well as phono-cardio graphic (PCG) monitors to capture fetal heart activity. The PCG signal contains some noise,

International Journal on Recent and Innovation Trends in Computing and Communication
ISSN: 2321-8169 Volume: 10 Issue: 10
DOI: https://doi.org/10.17762/ijritcc.v10i10.5732
***Article Received**: 28 July 2022 **Revised**: 05 September 2022 **Accepted**: 12 September 2022*

which is unavoidable during the acquisition procedure. ECG signal, may eliminate part of the PCG noise. Because the PCG information in the data set has a frequency of 0-2 kHz, many single-sample PCG waveforms are also larger in duration, hence down-sampling is performed first to lower the frequencies to below 1khz.. The peak signal appears less in the data set utilized in this experiment, but because the running time of this approach for eliminating spikes is minor, the practical test does not require much time and is also reserved.

For the 1st time, an unique tailored framework was suggested in [16] to address specific specificity within PCG signals. A clustering algorithm using age statistics with characteristics was devised to separate patients in order to remove individual differences at the source. Then, to create an individually customized diagnostic strategy, we constructed various classification models for distinct subgroups, thus attenuating the impact of individual specificity.

In [17], an innovative fusion design for heart beats categorization is suggested. Instead employing only one domain's data, general frequency and Mel domain characteristics are retrieved out from heartbeat. Multi-modal CNN fused structure separately using map generated by multiple feature extraction methods. Such feature maps are therefore blended in order to optimize the various retrieved features.

In [18], an empirical mode decomposition (EMD)-based signals refinement strategy is described to retrieve appropriate fetal heart rate style of communication (FHR). Following that, The PCG signal contains some noise, which is unavoidable during the acquisition procedure. The Schmidt's approach for eliminating signal spikes is mostly for PCG signals. The peak signal appears less in the data set utilized in this experiment, but because the running time of this approach for eliminating spikes is minor, the practical test does not require much time and is also reserved.

To aid clinicians in making correct judgements on suspected CAD patients, [19] provides optimum detection algorithms for suspected CAD detection based on variations in medical conditions. The electrocardiogram (ECG) as well as phonocardiogram (PCG) information involving Thirty CAD patients and thirty individuals There is currently no commonly accepted optimum PCG segmentation method, although with continuous ECG recordings, because of resilience. References show that multi-modal characteristics are useful in predicting CVDs. While facing high features in a multi-modal situation, however, feature selection stages are unavoidable. As a result, we require an efficient solution to tackle the dimension reduction problem. The optimum feature subset was then obtained using a heterogeneous feature selection (HFS) strategy that includes similarity matrix, sequential backward removal.

[20] present a low-cost real-time approach for diagnosing cardiac problems. Using Phonocardiogram (PCG) signal, we propose an integrated automated multimodal heart disease categorization (AMHDC) system. To do this, we first created an advanced fusion approach that makes use of pre-processing methods like Data Normalization as well as Data Augmentation. Second, we retrieved heart sound spectrograms and utilized them as feature and picture.

Survey on machine learning based prediction

The goal of this study, according to [21], aims to recognize cardiac arrhythmias using PCG signal, CNN or VGG16 algorithms, as well as classification techniques and visual pixel synthesis. For improved efficiency, phonocardiography (PCG) is additionally being explored. The bulk of arrhythmia categorization and detection approaches rely on surface Information extraction. To improve the effectiveness of cardiac diagnostics, a wavelet analysis approach at various resolutions is devised, incorporating temporal and wavelet.

In this study, information from 2319 patients were collected first based on the SOFA score. 4 commonly used machine learning (ML) methods were chosen and used to develop a real-time simulation tool for MODS based on full parameters (laboratory, drug, and non-invasive parameters, totaling 57 parameters) and non-invasive specifications only (17 parameters), and compared to four traditional scoring systems.

For the first time, a novel CAD identification method based on CMR pictures was developed, utilizing deep neural network feature extraction capabilities and merging the features with the assistance of a random forest. Image data must be converted to numeric qualities before they can be utilized in decision tree nodes. To do this, the predictions of many hold neural network convolutions (CNNs) are used as input qualities for selection trees. Because CNNs can represent picture data, our technique provides a universal classification strategy that can be used to any image data-base.

In [24] Data fusion, which combines data from several sources using ML and DL techniques, is gathering steam in medical applications. In this paper, we examine present study on how the most modern data fusing technologies are bringing clinical and scientific advancements in the field of cardiology. Doctors and scientists will be able to deliver more rapid, efficient, as well as accurate clinical services in the diagnosis and

International Journal on Recent and Innovation Trends in Computing and Communication
ISSN: 2321-8169 Volume: 10 Issue: 10
DOI: https://doi.org/10.17762/ijritcc.v10i10.5732
***Article Received**: 28 July 2022 **Revised**: 05 September 2022 **Accepted**: 12 September 2022*

treatment of cardiovascular disorders (CVD) using all of these modern information fusion capabilities.

Researchers developed Multi-Layer Acoustic Neural (MLAN) Systems to identify RHD symptoms utilizing heartbeat sounds and electrocardiogram (ECG) data in [25]. To improve accuracy in this proposed MLAN technology, novel methodologies such as multi-attribute acoustic appropriate sampling methods, cardiac sound sampling techniques, ECG information sampling procedure, and Acoustic Support Vector Machine (ASVM) are used.

[26] present a novel multi-modal method for forecasting CVDs depending on ECG as well as PCG features. We reconstruct ECG as well as PCG properties using traditional neural networks. To identify the best subset of features, the aggregated traits are evaluated to use an evolutionary algorithm. The support vector machine is then used to implement classifications.

The main goal of researchers utilizing ML Framework-A is on feature-selection and feature-classification, whereas feature extraction is an important stage in Framework-B and C. Raw ECG or PCG is useless unless the appropriate characteristics and parameters are calculated. Finding hidden characteristics in bio-signals is a difficult undertaking since they occur in a variety of complicated forms. Because signal analysis is a similar topic, With slight variations in feature extraction, ECG and PCG are incorporated in the same ML Framework. Segments, QRS period, average of Intervals, and mean difference of consecutive RR intervals are some common characteristics in ECG, where PCG impulses are assessed for either wavelet transform, spectral analysis, or time and frequency domains. Recent studies employ envelopes and length features to separate heart sounds, which improves heart disease prognosis. SVM and ANN important duties ECG interpretation. Deep neural networks, as per latest trend, excel in PCG classification. Deep neural networks also have outperformed cardiovascular tomography in terms of detecting heart disease. Deep neural networks excel in PCG as well as cardiovascular ultrasound classification. Although there are several data repositories and machine learning approaches accessible for heart disease detection, there is always room for advancement in levels of accuracy and other performance indicators.

System model

The following modules are included in the overall diagnostic system: noise reduction and spikes reduction, extraction of features, and model classification. Power frequency interfering, electromyography interruption, and baseline drift are all characteristics of noise. A multimodal feature extraction approach with matching contains thirty six time domain characteristics like variance and mean of the ECG and PCG intervals and magnitude, thirty six frequency domain samples are considered on Hamming window and discrete time Fourier transform, and fifty two MFCC coefficient elements. The semi hidden morkov model classification models are utilized here for these characteristics. Figure 1 gives overall structure of categorization system.

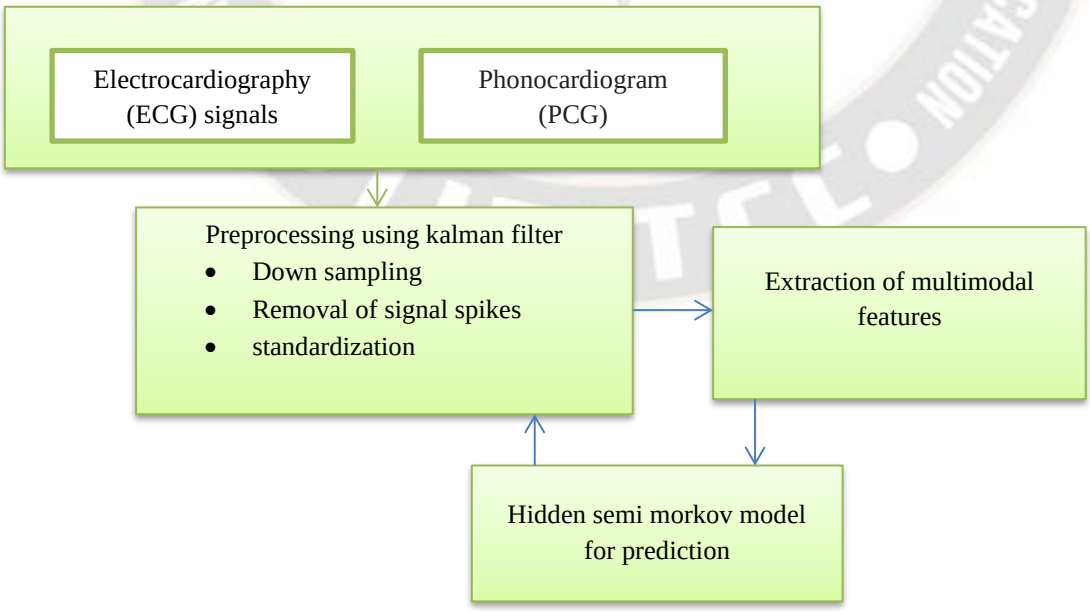

Figure-1 system model for heart disease prediction

International Journal on Recent and Innovation Trends in Computing and Communication
ISSN: 2321-8169 Volume: 10 Issue: 10
DOI: https://doi.org/10.17762/ijritcc.v10i10.5732
***Article Received**: 28 July 2022 **Revised**: 05 September 2022 **Accepted**: 12 September 2022*

The PCG signal contains some noise, which is unavoidable during the acquisition procedure. The kalman filter, such as the ECG signal, may eliminate part of the PCG noise. Because the PCG information in the data set has a frequency of 0-2 kHz, many single-sample PCG waveforms are also larger in duration, hence down-sampling is performed first to lower the frequencies to below 1khz. The Kalman filter is then employed to eliminate the signal's low frequencies, i.e., impulses below 25 Hz and signals over 400 Hz, ensuring that critical information is kept while efficiently eliminating most of the noise. Some signal spikes in the PCG signal may interfere with model categorization. Schmidt's approach for eliminating signal spikes is mostly for PCG signals. The peak signal appears less in the data set utilized in this experiment, but because the running time of this approach for eliminating spikes is minor, the practical test does not require much time and is also reserved.

Linear Quadratic Estimation (LQE), commonly called Kalman filtering in control theory and analytics, is a method that use a series of observations, which includes errors and gives estimation of undefined factors that correct than those observed just for a 1st time slot by estimating a joint distribution of probabilities across the variable. Closer look into filter reveals that the speech-signals are treated as a pth degree Auto-Regressive models. The present state sampling x(k) is determined by:

$$x(k)=\sum_{i=1}^{p} a_i x(i-k)+u(k) \qquad (1)$$

$$\begin{bmatrix} x(k-p+1) \\ x(k-p+1) \\ \vdots \\ x(k) \end{bmatrix} \sum_{i=1}^{n} X_i^2 = \begin{pmatrix} 0 & 1 & 0.....0 \\ 0 & 0 & 1.....0 \\ a_p & a_{p-1} & a_{p-2}.....a_{-1} \end{pmatrix}$$

$$\begin{bmatrix} x(k-p) \\ x(k-p+1) \\ \vdots \\ x(k-1) \end{bmatrix} + \begin{bmatrix} 0 \\ 0 \\ \vdots \\ 1 \end{bmatrix} \text{u(k)} \qquad (2)$$

$$X(K)=\Phi X(K-1)+Gu(k) \qquad (3)$$

where $X(k)$ is the $(pX1)$ vector matrix, Φ is matrix(pXp) represent state transition using LPC co-efficient calculating noisy-speeches based on equation (3.3), $u(k)$ gives incoming noise in k^{th}instant, and G gives $(pX1)$ input matrix.

When ECG and PCG is noise corrupted, the output $y(k)$ is:

$$y(k) = x(k) + w(k) \qquad (4)$$

here $w(k)$ gives noise with "0" variance / mean.

In vector form, $y(k) = HX(k) + w(k)$, here H gives $(1Xp)$ observation matrix denotedas H= [0 0….. 0 1]. Kalman filter gives $\hat{X}(k|k)$ This reflects the estimated state vector X(k), assuming distorted audio is captured up to k instants using the formulae presented below:

$$\hat{X}(k|k-1) = \phi\hat{X}(K-1|K-1) \qquad (5)$$

$$P(k|k-1) = \phi\hat{P}(K-1|K-1)\phi^T + GQG^T \qquad (6)$$

$$K(k) = P(K|K-1)H^T\big(HP(K|K-1)\big)H^T + R)^{-1} \qquad (7)$$

$$\hat{X}(k|k) = \hat{X}(k|k-1) + K(k)(y(k) - H\hat{X}(K|K-1)) \qquad (8)$$

$$P(k|k) = (I - K(k)H)P(k|k-1) \qquad (9)$$

Here,

- $\hat{X}(k|k-1)$ is an a priori estimation of the current condition vector $X(k)$.
- $P(k/k-1)$ yields the error covariance matrix of the priori estimation, which is provided by $E[ekekT\,]$ here $ek = X(k) - \hat{X}(k|k-1)$
- Q represents the noise covariance acquired for the procedure as a matrix. Likewise, R is the noise covariance measurement matrix, that is $2w$.
- The probability estimation of the vector field is given by $\hat{X}(k|k)$. The last element of $\hat{X}(k|k)$ in this situation is $\hat{x}(k)$, which yields the evaluation results of both the packaged speech signal.
- $P\,(k|k)$ returns the matrix expressing the errors correlation of an a posteriori estimate, gives $E[ekekT\,]$ here $ek = X(k) - \hat{X}(k|k)$.
- Let $\hat{X}(0|0) = [y(1)\ \cdots\ y(p)]$ and $P\,(0|0) = \sigma\ 2\ wI$, where I denotes $(p \times p)$ identity matrix.
- $N(k)$ is the strength of the Proposed method at the k^{th} instant.
- Expression $y(k) = H\hat{X}(k|k-1)$.

As a result, the equations of the Kalman filter are as follows: The Kalman gain $K(k)$ is chosen to minimize overall posterior error covariance, $P\,(k|k)$. K(k) falls as $P\,(k|k-1)$ lowers. Inspection reveals that when $K(k)$ drops, the faith in the posterior estimation process is greater than the trust in the noisy measurement.

Multimodal feature extraction process

The cardiac cycle is crucial in the categorization of heart sounds. For ECG and PCG data, one frequent estimate approach is envelope extraction. We do not directly recover

International Journal on Recent and Innovation Trends in Computing and Communication
ISSN: 2321-8169 Volume: 10 Issue: 10
DOI: https://doi.org/10.17762/ijritcc.v10i10.5732
***Article Received**: 28 July 2022 **Revised**: 05 September 2022 **Accepted**: 12 September 2022*

the envelope out from original ECG and PCG signal; rather, we recover the envelope of the selected IMF after applying EMD to the PCG signal. The EMD iterative filtering procedure separates the IMFs of every ECG and PCG signal, which is ordered by frequency between high to low. The essential characteristics of the heart sound have a frequency range of 50-200 Hz, located at the center of the overall signal frequency range. As a result, in most circumstances, the 2nd or 3rd IMF component is chosen as the best IMF component to reflect the matching PCG signal. The 2nd IMF of every ECG and PCG signals is selected for further investigation in this research. The tested ones representations will be utilized to facilitate more information in the suggested technique and modes of expression. Given x_1 to x_n are a set of vectors, so:

$$(x_1; x_2; \dots x_n) = \begin{matrix} x_{11} & x_{12} \dots & x_{1n} \\ x_{21} & x_{22} & x_{2n} \\ x_{n1} & x_{n2} & x_{n3} \end{matrix} \quad (10)$$

$$(x_1; x_2; \dots x_n) = \begin{matrix} x_{11} & x_{21} \dots & x_{n1} \\ x_{21} & x_{22} & x_{n2} \\ x_{1n} & x_{n2} & x_{nn} \end{matrix} \quad (11)$$

Given x is a vector, a is a scalar then:

$$X.a = \begin{matrix} ax_{11} & ax_{21} \dots & x_{n1} \\ ax_{21} & ax_{22} \dots & x_{n2} \\ ax_{1n} & ax_{n2} \dots & x_{nn} \end{matrix} \quad (12)$$

A Fast Fourier transform for vector x is represented by $FFT(x)$. As previously stated, we applied FMFE in three dimensions. As a result, three matching templates are required. The source of template is the ECG and PCG. As full ECG and PCG in our dataset is made up of three cycles. The template signal (m) in dimensions is easily calculated by averaging all three cycles (h_1, h_2, h_3) of 1 signal.

$$m = \frac{h_1, h_2, h_3}{3} \quad (13)$$

The template signal (m) is computed inside the dimensions for self-matching and frequency response as well as mutual matching in frequency domain by average of FFT) in all three cycles h_1, h_2, h_3 of one signal:

$$m = \frac{\|FFT(h_1)+FFT(h_2)+FFT(h_3)\|}{3} \quad (14)$$

It is worth noting that in frequency domain mutual matching, h_1, h_2, h_3 are the three portions of one specific regular ECG as well as PCG. The cardiac cycle is crucial in the categorization of heart sounds. For ECG and PCG data, one frequent estimate approach is envelope extraction. We do not directly recover the envelope out from original ECG and PCG signal; rather, we recover the envelope of the selected IMF after applying EMD to the PCG signal. The EMD iterative filtering procedure separates the IMFs of every ECG and PCG signal, which is ordered by frequency between high to low as $(w_1; w_2; \dots w_N)$. Gaussian wavelets were employed in this investigation. These represent gaussian 1st – 8th high derivative filter wavelets with N wavelet hyper-parameters. By convolution the pattern signal only with initial flter matrix, the template features may be retrieved.

$$X = m \otimes \mathrm{W} = (\mathrm{m} \otimes w_1; m \otimes w_2; \dots\dots; m \otimes w_N) \quad (15)$$

However, not all of the template characteristics are normally need to be taken into account. Since the same kind, in most circumstances, the 2nd or 3rd IMF component is chosen as the best IMF component to reflect the matching PCG signal. The 2nd IMF of every ECG and PCG signals is selected for further investigation in this research. The tested ones representations will be utilized to facilitate more information in the suggested technique and modes of expression. Given x_1 to x_n are a set of vectors. A fuzzy matching concept is suggested here to reduce overfitting. We believe that the maximum correlation energy is found in the same sort of heart sound signal. To identify correlation energy characteristics, matched filter matrix depending on greatest correlation is created. For improving first filter W, we utilize a mask U:

$$U = (\beta_1, \beta_2, .. \beta_0) \quad (16)$$

The maximum confidence c_ω is used to assess signal quality. To establish an overall categorization for a particular patient on several individual recordings, we use a basic criteria similar to what a doctor would employ when hearing to multiple places on the chest. The transmitting matrix A and the original state distributions were both invariant, as shown below.

$$W' = U^T W = (w_1', w_2', \dots w_0')$$

where $w_1'; w_2';\dots; w_0'$ provides improved O filter (O improves filters, quantity is 1 of the proposed technique's O hyper - parameters.) Fuzzy characteristic of template signals (X_m) and of target signal (X_s) may be derived in the same way

$$X_m = m \otimes W' = (m \otimes w_1'; m \otimes w_2' \dots\dots; m \otimes w_0') = (x_{m1}; x_{m2}; \dots . x_{m0}) \quad (17)$$

$$X_s = s \otimes W' = (\mathrm{s} \otimes w_1'; s \otimes w_2' \dots\dots; s \otimes w_0') = (x_{s1}; x_{s2}; \dots . x_{s0}) \quad (18)$$

International Journal on Recent and Innovation Trends in Computing and Communication
ISSN: 2321-8169 Volume: 10 Issue: 10
DOI: https://doi.org/10.17762/ijritcc.v10i10.5732
***Article Received**: 28 July 2022 **Revised**: 05 September 2022 **Accepted**: 12 September 2022*

In this study, we employ PCG information in the data set has a frequency of 0-2 kHz, many single-sample PCG waveforms are also larger in duration, hence down-sampling is performed first to lower the frequencies to below 1khz.. Schmidt's approach for eliminating signal spikes is mostly for PCG signals. The peak signal appears less in the data set utilized in this experiment, but because the running time of this approach for eliminating spikes is minor, the practical test does not require much time and is also discovered.mmd. These values are referred as $e_{s1}, e_{s2}, \ldots . e_{s0}$ in a vector ME

$$ME = (e_{s1}, e_{s2}, \ldots . e_{s0})$$

Every optimized wavelet provides a correlation energy content, resulting in a total of O energy characteristics in a single cardiac cycle. Since signal provides data from 1 cycle of every ECG and PCG signals, three PCG cycles in our investigation should have three layers of matching characteristics. The approach described above is used to extract matching degree and matching energy characteristics for each cycle. This indicates that each cardiac sound wave retrieved three (O + 1) matching characteristics in 1D of matching calculation. 1 full ECG and PCG signal may be described in the time domain as follows:

$$TD.S.MD = (mmd_1^{TDS}, mmd_2^{TDS}, mmd_3^{TDS}) \quad (19)$$

$$TD.S.MD = (ME_1^{TDS}, ME_2^{TDS}, ME_3^{TDS}) \quad (20)$$

The approach for extracting self-matching energy characteristics with freq., response identical to 1 described before. Distinction would be that the vibration signals utilizing FFT, and template signal is provided in Eq (21). We could create the result of having expression using the same way.

$$FD.S.MD = (mmd_1^{FDS}, mmd_2^{FDS}, mmd_3^{FDS}) \quad (21)$$

$$FD.M.MD = (mmd_1^{FDM}, mmd_2^{FDM}, mmd_3^{FDM}) \quad (22)$$

$$FD.S.ME = (ME_1^{FDS}, ME_2^{FDS}, ME_3^{FDS}) \quad (23)$$

$$FD.M.ME = (ME_1^{FDM}, ME_2^{FDM}, ME_3^{FDM}) \quad (24)$$

The frequency domain self-matching degree characteristic of 1 full cardiac sound signal is denoted by FD.S.MD, while the frequency domain self-matching energy characteristics are denoted by FD.S.ME. Mutual matching degree as well as mutual matching energy characteristics are denoted by FD.M.MD and FD.M.ME, respectively.

Prediction using Hidden semi morkov model

Figure 2 depicts a schematic of the mathematical model employed in this work. The system is represented as a set of variables S_i which represent the various actions in this context. For the time D_i, which would be a random variable, the system will remain in a certain state. The process then moves to another state, forming a Markov chain. The transition matrix is formed by the transition parameters $\pi_{i,j}, i, j = 1,2, \ldots n$, here $\pi_{i,j}$ denotes the probability of transformation from state i to the state j. Each state S_i is made up of D_i observations y. The transition probabilities $\pi_{i,j}$ are used to represent state transitions. The entire observation time is denoted by T.

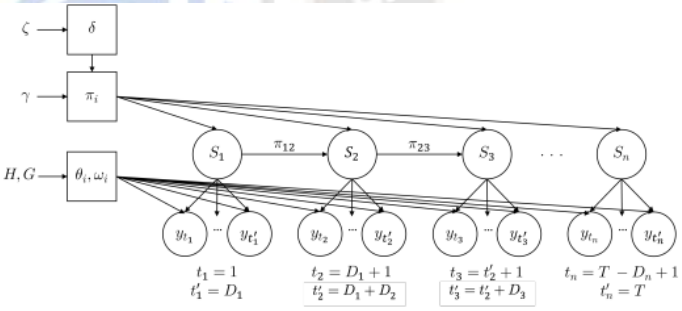

Figure 2. The hidden semi-Markov model

The HSMM is a hidden Markov model extension that explicitly represents the period of every state. Our method employs four simultaneous HSMMs with distinct signal classifications (ω1,..., ω4):

(ω1): Healthy normal signal- A 4-state segmentation model that excludes the RNN murmur posterior.

(ω2) Holosystolic murmur-The murmuring posterior substitutes the systole posterior in this four-state segmentation scheme.

(ω3) Early-systolic murmur- A 5-stage segmentation model in which the transition matrix necessitates a transition from the S1 state to the murmuring state and subsequently to the systolic state.

(ω4) systolic murmur-As previously stated, the model initially changes from S1 to systole.

International Journal on Recent and Innovation Trends in Computing and Communication
ISSN: 2321-8169 Volume: 10 Issue: 10
DOI: https://doi.org/10.17762/ijritcc.v10i10.5732
***Article Received**: 28 July 2022 **Revised**: 05 September 2022 **Accepted**: 12 September 2022*

The projected classification is determined by computing a segmented confidence c_ for each model and following its Viterbi state path., $q'^{(\omega)}_{1,T}$ through the posteriors:

$$c_\omega = \frac{\frac{1}{T}\sum_{t=1}^{T} P(q_t = q'^{(\omega)}_t}{x1} : T, R \qquad (25)$$

$$\omega' = argmax(c_\omega) \qquad (26)$$

The maximum confidence c_ω is used to assess signal quality. To establish an overall categorization for a particular patient on several individual recordings, we use a basic criteria similar to what a doctor would employ when hearing to multiple places on the chest. The transmitting matrix A and the original state distributions were both invariant, as shown below.

$$\pi = \{\tfrac{1}{4}, \tfrac{1}{4}, \tfrac{1}{4}, \tfrac{1}{4}\} \qquad (27)$$

Generating the hidden layer sequences for a fresh heartbeat with the existing parameter for HSMM was the HSS task. As a result, we may utilize a dynamic programming approach, notably the Viterbi algorithm, to tackle this type of issue. We denoted the overall series length as N, the quantity of hidden stages as H, the real state at period t as q t, the total true state sequential as Q, as well as the observing sequence as $O(t) = [O1, O2, \cdots, ON]$, here $O(t)$ denotes features at time point t. Formula for $\delta_t(j)$ is,

$$\delta_t(j) = \max(d)\left[\max(i \neq j)[\delta_{t-d}(i).a_{ij}\right].p_j(d).\prod_{s=0}^{d-1} b_j(O_{t-s})] \qquad (28)$$

where $\delta_t(j)$ is likelihood for 1st t observations and ends in state j at time t, having $1 \leq i, j \leq H, 1 \leq t \leq N, 1 \leq d \leq d_{max}$ and d_{max} is set as the duration of a complete heartbeat time and $\delta_t(j) = \pi_j b_j(O1)$ To determine the best path for the complete heart sound, calculate the maximum of $\delta_t(j)$) in the range $N \leq t \leq N + d_{max} - 1$. When defining q t* as the hidden layer determined by the method again for final position sequence at time point t,1 t N, this highest value was used to determine the internal state q N*. 'Murmur Present' is predicted if one of the impulses are identified as a murmur. If this is not the case, and Cw for any message falls below a certain threshold (0.65), the value 'Unknown' is anticipated. 'Murmur Absent' is predicted otherwise.

Performance analysis

Dataset description- PhysioNet/CinC Challenge 2016 ECG and PCG data were utilized in this investigation [27]. Several foreign institutes have supplied datasets. Several institutions claim that the dataset is divided into six subgroups labelled 'training-a' through 'training-f.' The PCG signal contains some noise, which is unavoidable during the acquisition procedure. The kalman filter, such as the ECG signal, may eliminate part of the PCG noise. Because the PCG information in the data set has a frequency of 0-2 kHz, many single-sample PCG waveforms are also larger in duration, hence down-sampling is performed first to lower the frequencies to below 1khz. The Kalman filter is then employed to eliminate the signal's low frequencies, i.e., impulses below 25 Hz and signals over 400 Hz, ensuring that critical information is kept while efficiently eliminating most of the noise. Some signal spikes in the PCG signal may interfere with model categorization. Schmidt's approach for eliminating signal spikes is mostly for PCG signals.

Evaluation criteria-:For quantifying classification findings, we use 5 assessment measures, namely accuracy (ACC), sensitivity (SN), , F-score, specificity (SP) with receiver operating characteristic (ROC), to compare performance across instances, defined as:

$$\boldsymbol{SN} = \frac{\boldsymbol{TP}}{\boldsymbol{TP} + \boldsymbol{FN}}$$

$$\boldsymbol{SP} = \frac{\boldsymbol{TN}}{\boldsymbol{TN} + \boldsymbol{FP}}$$

$$\boldsymbol{F - score} = \frac{\boldsymbol{2 \times P \times SN}}{\boldsymbol{P + SN}}$$

$$\boldsymbol{ACC} = \frac{\boldsymbol{TP + TN}}{\boldsymbol{TP + FP_{TN} + FN}}$$

True negative, false positive, false negative, true positive, and precision values are denoted by TP, FN, FP, TN, and P. The ROC curve may be used to assess screening procedures and prediction systems. The area below the ROC curve represents the tradeoff among SN and SP (AUC).

Table-1 analysis of sensitivity

Number of epochs	**CL-ECG-Net**	**CL-PCG-Net**	**LSTMs + PCA**	**LSTMs + GA**	**HSMM**
10	0.88	0.71	0.89	0.89	0.94
20	0.87	0.69	0.90	0.90	0.95
30	0.881	0.68	0.91	0.91	0.93
40	0.872	0.70	0.88	0.88	0.94
50	0.88	0.72	0.89	0.89	0.95

International Journal on Recent and Innovation Trends in Computing and Communication
ISSN: 2321-8169 Volume: 10 Issue: 10
DOI: https://doi.org/10.17762/ijritcc.v10i10.5732
***Article Received**: 28 July 2022 **Revised**: 05 September 2022 **Accepted**: 12 September 2022*

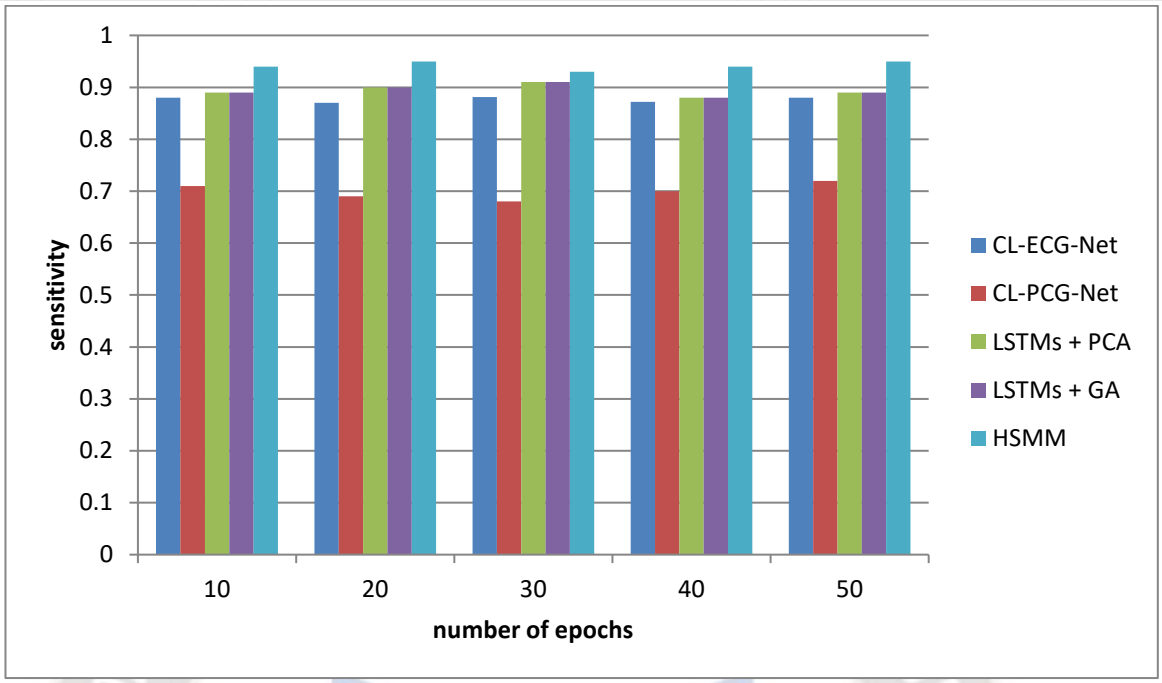

Figure-3 comparison of sensitivity

Figure 3 compares the sensitivity of current CL-ECG-Net, CL-PCG-Net, LSTMs + PCA, LSTMs + GA, and the novel HSMM technique. The X-axis illustrates the no., of epochs utilised for analysis, where Y-axis shows the % sensitivity values acquired. The CL-ECG-Net, CL-PCG-Net, LSTMs + PCA, and LSTMs + GA techniques had sensitivity values of 0.898, 0.711, 0.903, 0.903, and 0.952, respectively. In comparison, the suggested HSMM technique attained sensitivity of 0.952.

Table-2 analysis of specificity

Number of epochs	**CL-ECG-Net**	**CL-PCG-Net**	**LSTMs + PCA**	**LSTMs + GA**	**HSMM**
10	0.83	0.69	0.831	0.80	0.92
20	0.84	0.70	0.82	0.85	0.91
30	0.841	0.71	0.83	0.83	0.93
40	0.842	0.701	0.831	0.84	0.91
50	0.838	0.702	0.82	0.85	0.92

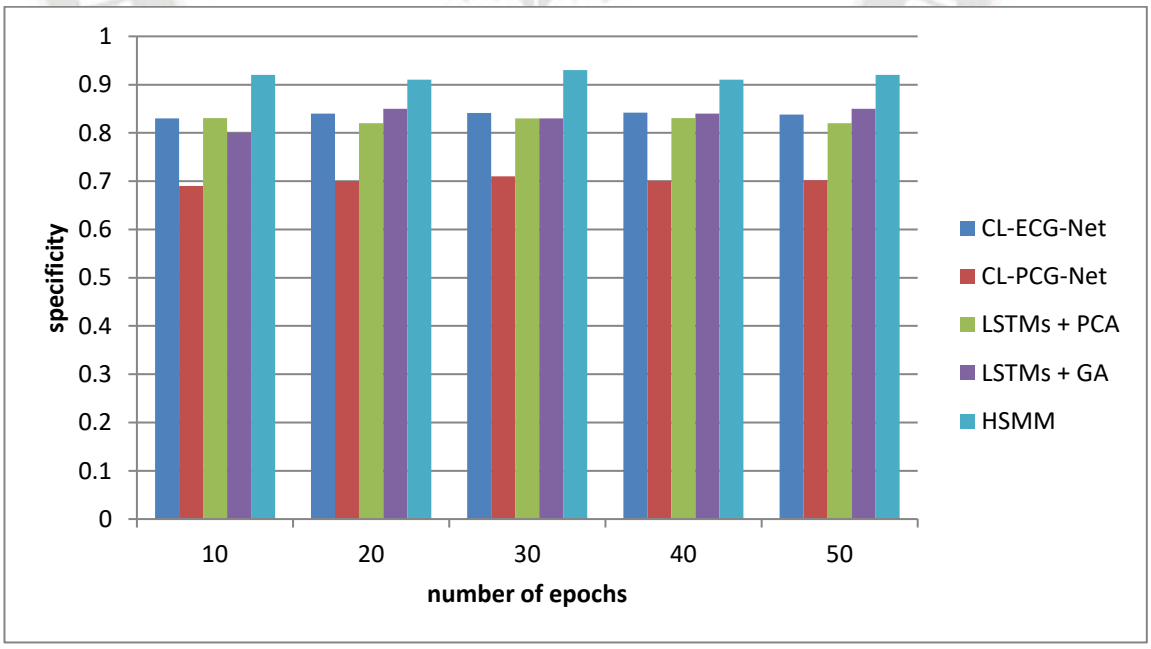

Figure-4 comparison of specificity

International Journal on Recent and Innovation Trends in Computing and Communication
ISSN: 2321-8169 Volume: 10 Issue: 10
DOI: https://doi.org/10.17762/ijritcc.v10i10.5732
***Article Received**: 28 July 2022 **Revised**: 05 September 2022 **Accepted**: 12 September 2022*

Figure 4 compares the specificity of current CL-ECG-Net, CL-PCG-Net, LSTMs + PCA, LSTMs + GA, and the proposed HSMM technique. The X-axis shows the no., of epochs utilized for analysis, where Y-axis shows the % specificity values acquired. The CL-ECG-Net, CL-PCG-Net, LSTMs + PCA, and LSTMs + GA techniques had specificities of 0.847, 0.70, 0.83, 0.85, and 0.92, respectively. In comparison, the suggested HSMM technique attained a specificity of 0.92.

Table-3 analysis of F-score

Number of epochs	CL-ECG-Net	CL-PCG-Net	LSTMs + PCA	LSTMs + GA	HSMM
10	0.87	0.70	0.87	0.87	0.91
20	0.86	0.71	0.86	0.86	0.90
30	0.85	0.69	0.85	0.85	0.92
40	0.871	0.691	0.86	0.86	0.91
50	0.862	0.67	0.87	0.87	0.91

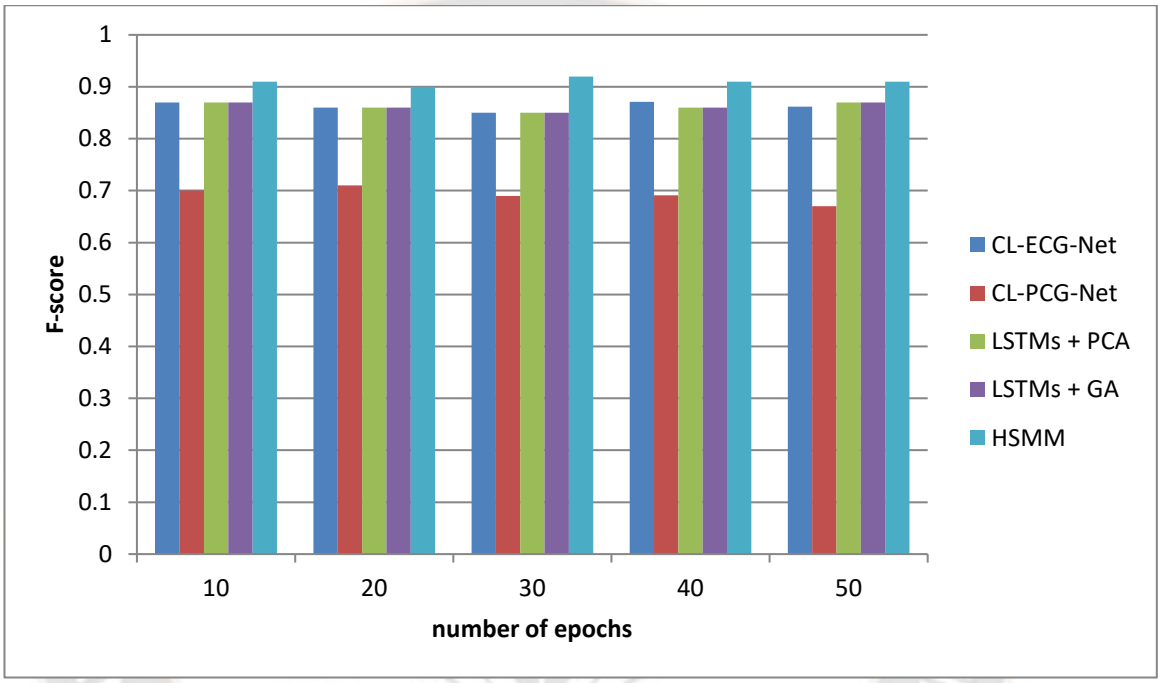

Figure-5 comparison of F-score

Figure 5 depicts the F-score comparison between the existing CL-ECG-Net, CL-PCG-Net, LSTMs + PCA, LSTMs + GA, and the new HSMM technique. The no., of epochs utilised for analysis is shown on the X-axis, and the F-score values produced in % are shown on the Y-axis. The F-scores for the CL-ECG-Net, CL-PCG-Net, LSTMs + PCA, and LSTMs + GA techniques were 0.873, 0.705, 0.871, and 0.874, respectively. In comparison, the suggested HSMM approach obtained an F-score of 0.94.

Table-4 analysis of ACC

Number of epochs	CL-ECG-Net	CL-PCG-Net	LSTMs + PCA	LSTMs + GA	HSMM
10	0.861	0.70	0.87	0.871	0.91
20	0.87	0.69	0.86	0.861	0.92
30	0.90	0.71	0.86	0.862	0.91
40	0.88	0.69	0.87	0.87	0.90
50	0.87	0.67	0.872	0.872	0.91

International Journal on Recent and Innovation Trends in Computing and Communication
ISSN: 2321-8169 Volume: 10 Issue: 10
DOI: https://doi.org/10.17762/ijritcc.v10i10.5732
***Article Received**: 28 July 2022 **Revised**: 05 September 2022 **Accepted**: 12 September 2022*

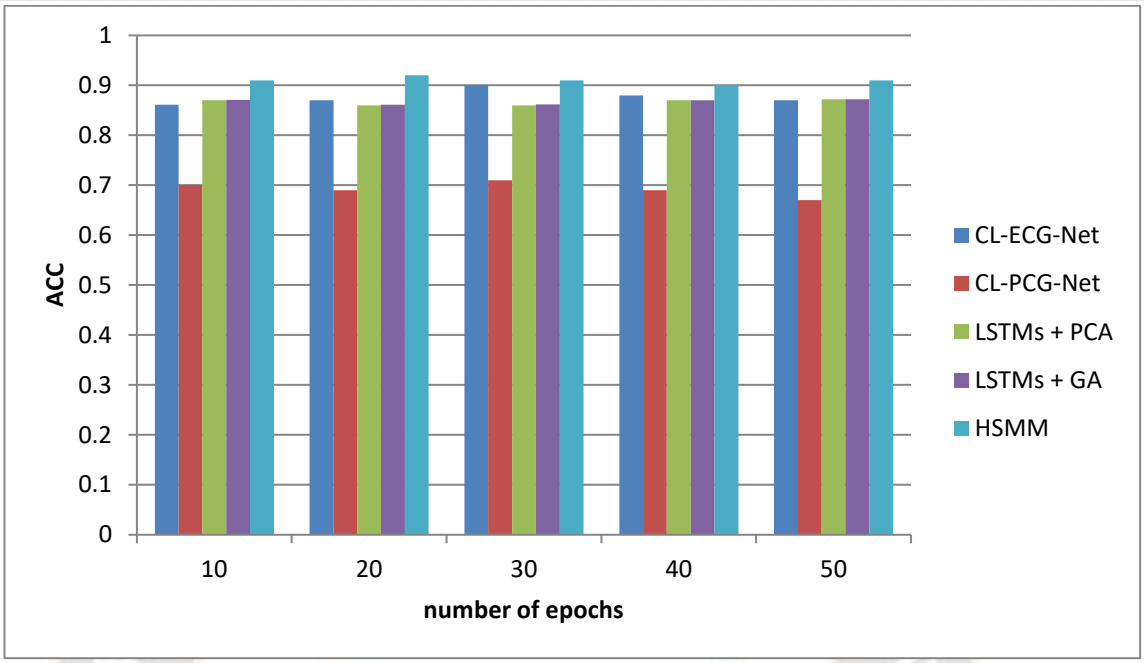

Figure-6 comparison of ACC

Figure 6 depicts an ACC comparison of current CL-ECG-Net, CL-PCG-Net, LSTMs + PCA, LSTMs + GA, and the novel HSMM technique. The X-axis shows the no., of epochs utilized for analysis, where Y-axis shows the % ACC values achieved. CL-ECG-Net, CL-PCG-Net, LSTMs + PCA, and LSTMs + GA approaches produced ACCs of 0.872, 0.709, 0.871, and 0.873, respectively. In comparison, the suggested HSMM technique obtained 0.91 of ACC.

Table-5 analysis of AUC

Number of epochs	**CL-ECG-Net**	**CL-PCG-Net**	**LSTMs + PCA**	**LSTMs + GA**	**HSMM**
10	0.91	0.74	0.91	0.92	0.94
20	0.92	0.73	0.92	0.91	0.95
30	0.89	0.72	0.89	0.93	0.96
40	0.90	0.74	0.90	0.92	0.95
50	0.91	0.73	0.91	0.91	0.96

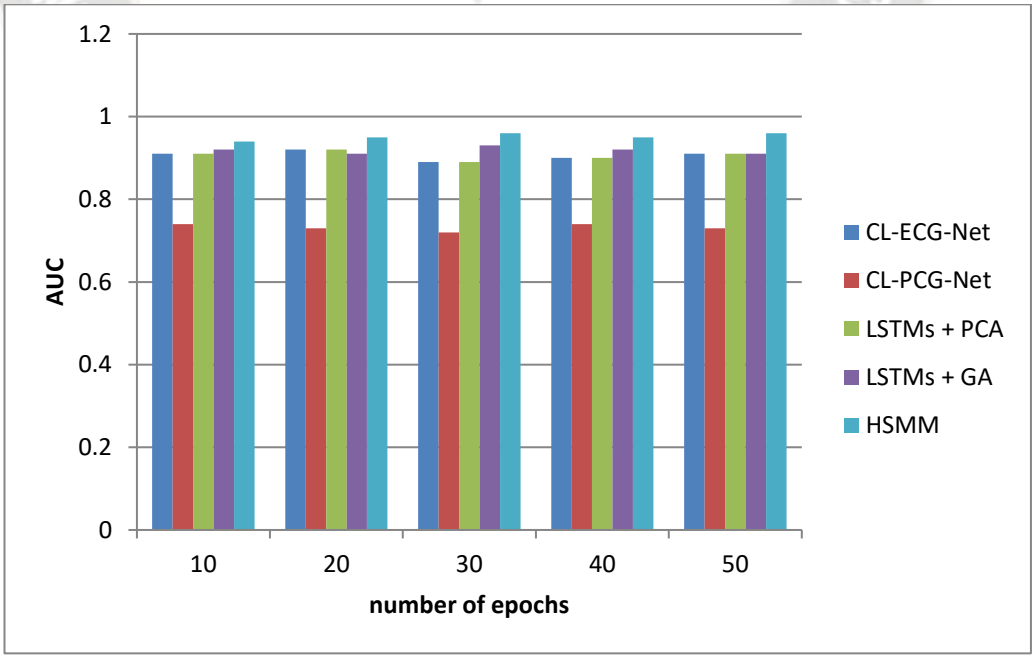

Figure-7 comparison of AUC

International Journal on Recent and Innovation Trends in Computing and Communication
ISSN: 2321-8169 Volume: 10 Issue: 10
DOI: https://doi.org/10.17762/ijritcc.v10i10.5732
***Article Received**: 28 July 2022 **Revised**: 05 September 2022 **Accepted**: 12 September 2022*

Figure 7 compares the AUC of existing CL-ECG-Net, CL-PCG-Net, LSTMs + PCA, LSTMs + GA, and the new HSMM methods. The X-axis shows the no.,r of epochs utilised for analysis, where Y-axis shows the % AUC values acquired. CL-ECG-Net, CL-PCG-Net, LSTMs + PCA, and LSTMs + GA approaches produced AUCs of 0.916, 0.748, 0.918, and 0.936, respectively. In comparison, the suggested HSMM technique achieved an AUC of 0.96.

Table- 6 Overall comparative analysis

Method	**SN**	**SP**	**F-score**	**ACC**	**AUC**
CL-ECG-Net	0.898	0.847	0.873	0.872	0.916
CL-PCG-Net	0.711	0.70	0.705	0.709	0.748
LSTMs + PCA	0.903	0.83	0.871	0.871	0.918
LSTMs + GA	0.903	0.85	0.874	0.873	0.936
HSMM	0.952	0.92	0.94	0.91	0.96

Conclusion

Here, in our work we suggested a multi-modal machine learning technique that integrates ECG and PCG to predict CVDs. From preprocessed pictures, we recovered ECG deep-coding characteristics. The genetic algorithm is used to iteratively screen the fused features to get the best feature subset for categorization. To produce the prediction, we used a hidden semi-morkov model classifier that was trained using the best feature subset. Our proposed strategy's categorization performance proves its efficacy. The findings also show that a multi-modal categorization beats competing single-modal techniques in predicting CVDs. Nonetheless, the networks used in this article have been optimized for the restricted datasets. There is a wealth of CAD data available in clinics. The suggested technique HSMM obtains sensitivity of 0.952, specificity of 0.92, F-score of 0.94, ACC of 0.91, and AUC of 0.96. The strategy we suggest can give a broad foundation for addressing the multi-modal challenge. In the future, we will collaborate with physicians to acquire more relevant data and improve our model.

Reference

[1]. Li M et al (2021) Piwi-interacting rnas (pirnas) as potential biomarkers and therapeutic targets for cardiovascular diseases. Angiogenesis 24(1):19–34

[2]. Bui AL, Horwich TB, Fonarow GC (2011) Epidemiology and risk profile of heart failure. Nat Rev Cardiol 8(1):30–41

[3]. Hassanin A, Hassanein M, Bendary A, Maksoud MA (2020) Demographics, clinical characteristics, and outcomes among hospitalized heart failure patients across different regions of egypt. Egypt Heart J 72(1):1–9

[4]. Allen LA et al (2012) Decision making in advanced heart failure: a scientific statement from the american heart association. Circulation 125(15):1928–1952

[5]. Yusuf S, Reddy S, Ounpuu S, Anand S (2001) Global burden of cardiovascular diseases: Part ii: variations in cardiovascular disease by specific ethnic groups and geographic regions and prevention strategies. Circulation 104(23):2855–2864

[6]. Das R, Turkoglu I, Sengur A (2009) Effective diagnosis of heart disease through neural networks ensembles. Expert Syst Appl 36(4):7675–7680

[7]. Arabasadi Z, Alizadehsani R, Roshanzamir M, Moosaei H, Yarifard AA (2017) Computer aided decision making for heart disease detection using hybrid neural network-genetic algorithm. Comput Methods Programs Biomed 141:19–26

[8]. Balaha HM, Ali HA, Saraya M, Badawy M (2021) A new arabic handwritten character recognition deep learning system (ahcrdls). Neural Comput Appl 33(11):6325–6367

[9]. Namejs Zeltins. (2022). Implementation of Shutdown Mode for the Boosting and Inverting Buck-Boost Converter. Acta Energetica, (03), 15–21. Retrieved from http://actaenergetica.org/index.php/journal/article/view/472

[10]. Chen AH, Huang SY, Hong PS, Cheng CH, Lin EJ (2011) Hdps: heart disease prediction system, In: 2011 computing in cardiology. IEEE, pp 557–560

[11]. Olmez, T. and Dokur, Z. (2003). Classification of heart ¨ sounds using an artificial neural network. Pattern Recognition Letters, 24(1-3):617–629.

[12]. Wang, X., Li, Y., Sun, C., and Liu, C. (2009). Detection of the first and second heart sound using heart sound energy. In 2009 2nd International Conference on Biomedical Engineering and Informatics, pages 1– 4. IEEE.

[13]. Zhong, L., Guo, X., Ji, A., and Ding, X. (2011). A robust envelope extraction algorithm for cardiac sound signal segmentation. In 2011 5th International Conference on Bioinformatics and Biomedical Engineering, pages 1–5. IEEE.

[14]. Kumar, D., Carvalho, P. d., Antunes, M., Henriques, J., Maldonado, M., Schmidt, R., and Habetha, J. (2006). Wavelet transform and simplicity based heart murmur segmentation. In 2006 Computers in Cardiology, pages 173–176. IEEE

[15]. Jacek Marecki, & Dr. Sunita Chaudhary. (2022). Electrical Structure for Embedded Commuter Vision for Automobile Sector. Acta Energetica, (02), 44–51. Retrieved from http://actaenergetica.org/index.php/journal/article/view/468

International Journal on Recent and Innovation Trends in Computing and Communication
ISSN: 2321-8169 Volume: 10 Issue: 10
DOI: https://doi.org/10.17762/ijritcc.v10i10.5732
***Article Received**: 28 July 2022 **Revised**: 05 September 2022 **Accepted**: 12 September 2022*

[16]. Zeng, Y., Yang, S., Yu, X., Lin, W., Wang, W., Tong, J., & Xia, S. (2022). A multimodal parallel method for left ventricular dysfunction identification based on phonocardiogram and electrocardiogram signals synchronous analysis. *Mathematical Biosciences and Engineering*, *19*(9), 9612-9635.

[17]. FAISANT, M., FONTECAVE-JALLON, J., GENOUX, B., RIVET, B., DIA, N., RESENDIZ, M., ... & HOFFMANN, P. (2022). Non-invasive fetal monitoring: Fetal Heart Rate multimodal estimation from abdominal electrocardiography and phonocardiography. *Journal of Gynecology Obstetrics and Human Reproduction*, 102421.

[18]. Huang, Y., Li, H., Tao, R., Han, W., Zhang, P., Yu, X., & Wu, R. (2022). A customized framework for coronary artery disease detection using phonocardiogram signals. *Biomedical Signal Processing and Control*, *78*, 103982.

[19]. Ranipa, K., Zhu, W. P., & Swamy, M. N. S. (2021, May). Multimodal CNN fusion architecture with multi-features for heart sound classification. In *2021 IEEE International symposium on circuits and systems (ISCAS)* (pp. 1-5). IEEE.

[20]. Shokouhmand, A., Antoine, C., Young, B. K., & Tavassolian, N. (2021, November). Multi-modal Framework for Fetal Heart Rate Estimation: Fusion of Low-SNR ECG and Inertial Sensors. In *2021 43rd Annual International Conference of the IEEE Engineering in Medicine & Biology Society (EMBC)* (pp. 7166-7169). IEEE.

[21]. Zhang, H., Wang, X., Liu, C., Liu, Y., Li, P., Yao, L., ... & Jiao, Y. (2020). Detection of coronary artery disease using multi-modal feature fusion and hybrid feature selection. *Physiological Measurement*, *41*(11), 115007.

[22]. Tariq, Z., Shah, S. K., & Lee, Y. (2020, December). Automatic multimodal heart disease classification using phonocardiogram signal. In *2020 IEEE International conference on big data (Big Data)* (pp. 3514-3521). IEEE.

[23]. Raghuram, S., Niyaz, T., Purma, H., Choubey, S. B., & Sreenivasulu, Y. Cardiac Arrhythmia Prediction and Prevention of Heart failure using PCG (PhonoCardioGram) and CNN.

[24]. Liu, G., Xu, J., Wang, C., Yu, M., Yuan, J., Tian, F., & Zhang, G. A Machine Learning Method for Predicting the Probability of Mods Using Only Non-Invasive Parameters. *Available at SSRN 4129902*.

[25]. Khozeimeh, F., Sharifrazi, D., Izadi, N. H., Joloudari, J. H., Shoeibi, A., Alizadehsani, R., ... & Islam, S. M. S. (2022). RF-CNN-F: random forest with convolutional neural network features for coronary artery disease diagnosis based on cardiac magnetic resonance. *Scientific Reports*, *12*(1), 1-12.

[26]. Amal, S., Safarnejad, L., Omiye, J. A., Ghanzouri, I., Cabot, J. H., & Ross, E. G. (2022). Use of Multi-Modal Data and Machine Learning to Improve Cardiovascular Disease Care. *Frontiers in Cardiovascular Medicine*, *9*.

[27]. Antony Kumar, K., & Carmel Mary Belinda, M. J. (2022). A Multi-Layer Acoustic Neural Network-Based Intelligent Early Diagnosis System for Rheumatic Heart Disease. *International Journal of Image and Graphics*, 2450012.

[28]. Li, P., Hu, Y., & Liu, Z. P. (2021). Prediction of cardiovascular diseases by integrating multi-modal features with machine learning methods. *Biomedical Signal Processing and Control*, *66*, 102474.

[29]. C. Liu, D. Springer, Q. Li, B. Moody, R.A. Juan, F.J. Chorro, F. Castells, J.M. Roig, I. Silva, A.E.W. Johnson, Z. Syed, S.E. Schmidt, C.D. Papadaniil, L. Hadjileontiadis, H. Naseri, A. Moukadem, A. Dieterlen, C. Brandt, H. Tang, M. Samieinasab, M. R. Samieinasab, R. Sameni, R.G. Mark, G.D. Clifford, An open access database for the evaluation of heart sound algorithms, Physiol. Meas. 37 (2016) 2181–2213, https://doi.org/10.1088/0967-3334/37/12/2181.

[30]. Syed Hassan, MIT Automated Auscultation System, 2005.

[31]. Z. Syed, D. Leeds, D. Curtis, F. Nesta, R.A. Levine, J. Guttag, A framework for the analysis of acoustical cardiac signals, IEEE Trans. Biomed. Eng. 54 (2007) 651–662,